

## Preliminary investigation of the effect of dimple size on friction in line contacts

Xiaolei Wang\*, Wei Liu, Fei Zhou, Di Zhu

Nanjing University of Aeronautics and Astronautics, 29# Yudao Street, Nanjing 210016, China

### ARTICLE INFO

#### Article history:

Received 13 July 2008

Received in revised form

28 February 2009

Accepted 20 March 2009

Available online 1 April 2009

#### Keywords:

Surface texture

Line contact

Friction

Load carrying capacity

### ABSTRACT

The scale of surface texture is becoming an important issue of surface texture design, particularly for the condition of low speed and high load. Experiments were carried out to investigate the effect of dimple size on friction under line contact condition. The patterns of dimples distributed as square array were fabricated on the surface of brass disks. Each pattern has the same area density of 7%, the same depth over diameter ratio  $h/d$  of 0.03, and dimple diameter  $d$  varying from 20 to 60  $\mu\text{m}$ . The frictional tests of the brass disk sliding against a stationary cylindrical surface of bearing roller were conducted. It was found that the pattern with dimple diameter of 20  $\mu\text{m}$  presented the effect of friction reduction. For the further understanding of the effect of dimple size under line contact condition, numerical simulations were also carried out to evaluate the hydrodynamic pressure within the contact of cylindrical and plane surfaces. The effects of dimple size and radius of the cylinder on the load carrying capacity were evaluated and discussed.

© 2009 Elsevier Ltd. All rights reserved.

### 1. Introduction

Through eons of life evolution, biological surfaces exhibit appealing and enigmatic properties for specific purposes. The longitudinal ribs on shark skin reduce drag and friction force dramatically. The micro- and nano-structures on lotus leaves represent self-cleaning surfaces to avoid fluid-dynamic deterioration by the agglomeration of dirt [1,2]. These nature facts remind people that a smooth surface is not always the best. The discovery that scored or marked golf ball flies farther inspired people to develop modern golf ball which is coated with dimpled enamel. However, this kind of approach could not be always successful without comprehensive understanding of the mechanisms, just as that developing aircraft needs mathematical expressions from aerodynamics rather than just watching the flight of bird.

The surface texture, such as micro-dimples or grooves, has been a well known approach to improve tribological performances of sliding surfaces. Reserving lubricant to prevent seizure should be the earliest understanding of the lubricating mechanism of surface texture. Hence, the cross hatch by honing has been successfully used for cylinder liner of combustion engine so far [3]. In the 1960s, Hamilton et al. indicated that micro-irregularities are able to generate the additional hydrodynamic pressure to increase the load carrying capacity of the surfaces [4]. This theory has been well accepted, and micro-hydrodynamic effect is

regarded as the most dominant effect of surface texture at the condition of high speed and low load. At this condition, the texture design concept is mainly according to fluid dynamics [5–10], and there is an optimal depth over diameter ratio similar to the case of step bearing.

At the “dry” contact condition, it is known the surface texture could trap wear debris to prevent further abrasive wear [11], and decreases the contact area to reduce the adhesive force between the disk and the slider of magnetic storage devices [12].

The condition with low speed and high load is complicated because full film lubrication could not be established easily. A part of the surface is in contact so that the friction was determined by how surface texture influences boundary lubrication [13], EHL, lubricant reservoir [14], and so on. Currently, lot of research works concentrated on this field. Dimples with the depth in nano-scale were reported to be effective for friction reduction at low speed and high load conditions [15]. The reason has been well explained by EHL experiments [16–18], which showed that a significant increase in lubricant film thickness is induced by a shallow micro-cavity in the elastohydrodynamic lubrication regime. However, beside the depth issue, it is still unclear what kind of surface texture is good for high load situation, and some results even conflicted. Wakuda et al. carried out the friction tests of line contact between steel cylinder and dimpled  $\text{Si}_3\text{N}_4$  ceramic plate [19]. His results suggested that the dimples with the diameter larger than Hertz contact width resulted in lower friction coefficient. Wang et al. proposed the method of virtual texturing to optimize the design of surface texture; the results suggested that the lubrication transitions from a highly hydrodynamic state

\* Corresponding author. Tel./fax: +86 25 84893630.

E-mail addresses: [xlei\\_wang@yahoo.com](mailto:xlei_wang@yahoo.com), [xl\\_wang@nuaa.edu.cn](mailto:xl_wang@nuaa.edu.cn) (X. Wang).

in the case of several large size dimples to a mixed state in the case of many small size dimples [20]. Meanwhile, Pettersson et al. conducted the friction tests between a bearing steel ball and textured silicon wafer [21]. She presented a figure which separated the surface patterns into two groups. One is the patterns resulted in low friction and no measurable wear, the other is the features resulted in high friction and severe wear. It is difficult to have a simple parameter to identify the difference of the patterns in these two groups. But, the image is that the features which caused low friction are smaller than that which caused high friction. Costa et al. investigated the influence of patterns of various shapes of depressions on lubrication film thickness by the reciprocating sliding of patterned plane steel surfaces against cylindrical counter bodies [22]. It is found that textured planes with features much larger than the elastic contact width obtained film thickness smaller than those of untextured specimen. So, smaller or larger, it is still disputable which is better for friction reduction in case of high contact pressure such as line contact.

This paper attempts to study the surface texture effect at the condition of line contact, particularly the issue of dimple size effect. Experiments were carried out to investigate the dimple size effect on the friction between cylindrical and plane surfaces. In order to understand the experimental results, numerical simulations based on micro-hydrodynamic effect were conducted to analyze the influence of dimple size and cylindrical radius on the load carrying capacity of the surfaces.

## 2. Experimental

### 2.1. Specimens and surface texturing

Cylindrical and plane specimens were used to perform sliding tests at line contact condition. The roller of SKF thrust rolling bearing 81208 was used as the cylinder. It has diameter of 9 mm and length of 8 mm. Fig. 1 shows the optical microscope image of the cylindrical surface.

Brass disks with diameter of 62.5 mm and thickness of 6 mm were used as the plane specimens. The disks were first ground and polished using Buehler<sup>®</sup> standard procedure to obtain the surface roughness of  $R_a$  around 0.03  $\mu\text{m}$ . Photolithographic technique was used to fabricate a photoresist mask on the surface of brass disk with a specific surface pattern of dimples. Then, the uncovered surface was electrolytic etched in 1 M NaCl solution with about

0.2 A DC current at room temperature. The depth of the depression was determined by etching time. After photoresist was removed by solvent, the disk surface was with the pattern of dimples and ready for test. Fig. 2 shows the optical microscope images of dimple patterns fabricated in this research. The dimples are arranged as a square array on the surface of each brass disk. The specific parameters of each pattern are listed in Table 1.

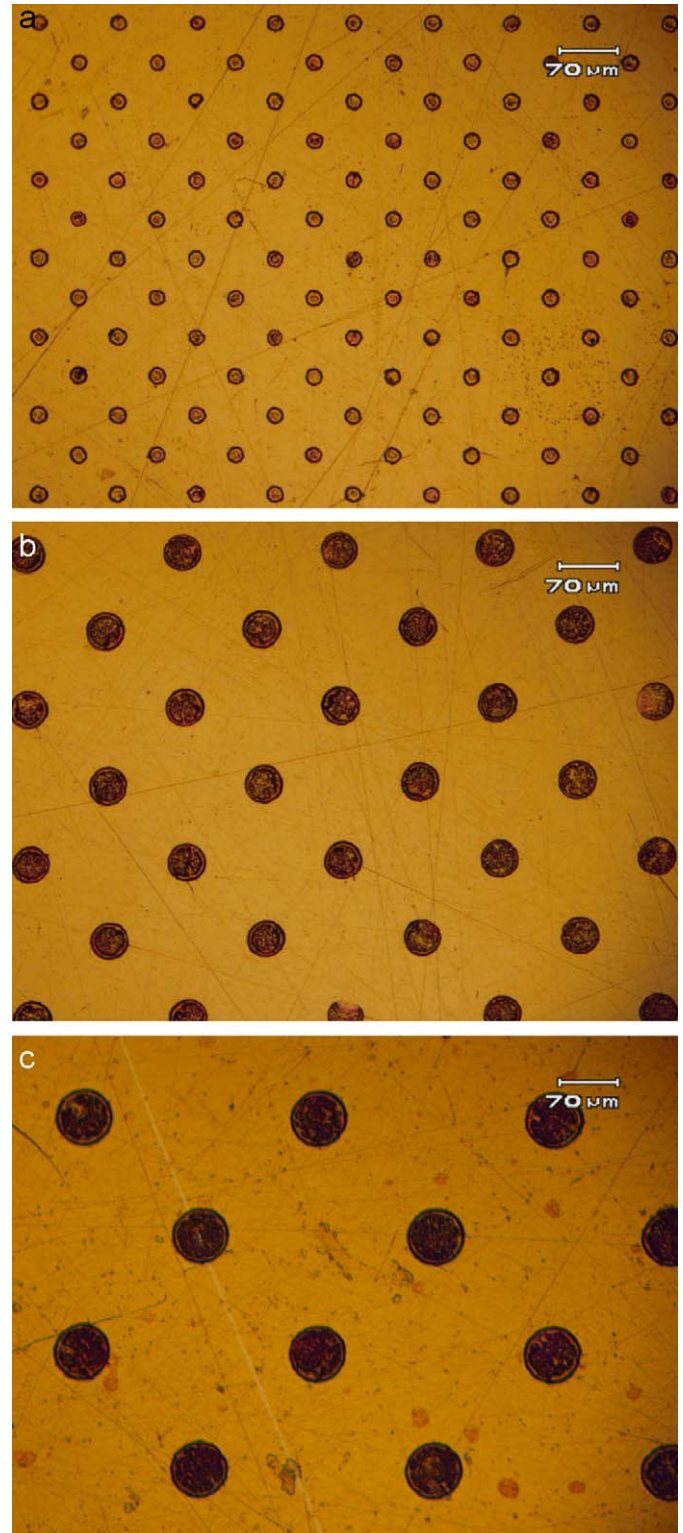


Fig. 2. Optical images of the patterns on the surface of brass disks. (a)  $d = 20 \mu\text{m}$ , (b)  $d = 40 \mu\text{m}$  and (c)  $d = 60 \mu\text{m}$ .

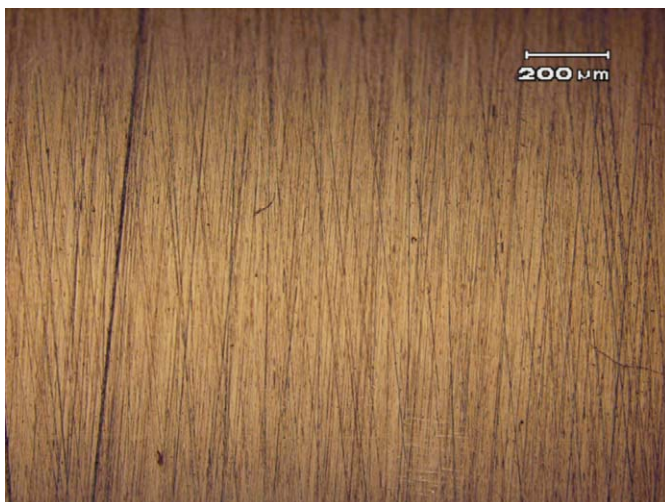
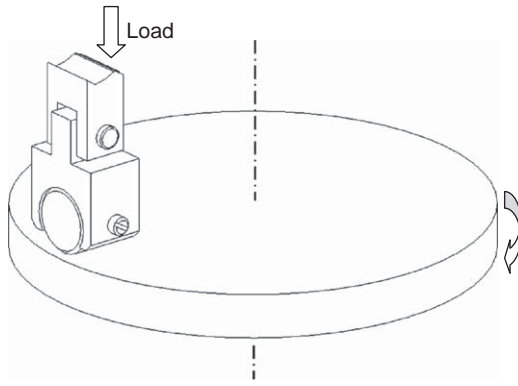


Fig. 1. Optical microscope image of the cylinder surface.

**Table 1**  
Features of the dimpled patterns.

Diameter $d$ ( $\mu\text{m}$ )	Area density $r$ (%)	Depth $h$ ( $\mu\text{m}$ )	Depth over diameter ratio $h/d$
60	7	1.8	0.03
40	7	1.2	0.03
20	7	0.6	0.03



**Fig. 3.** Schematic diagram of the friction test setting.

In order to focus on the effect of dimple size on friction, these patterns have the same area density  $r$  of 7%, and dimple diameters  $d$  of 20, 40, and 60  $\mu\text{m}$ . The depths  $h$  of the dimple varied according to the dimple diameter to obtain the same depth over diameter ratio  $h/d$  around 0.03, which was the optimal value for load carrying capacity of the parallel sliding surfaces reported in Ref. [7].

## 2.2. Tester and test procedure

The CSEM pin-on-disk tester was modified to enable a cylinder-on-flat test geometry. As shown in Fig. 3, the brass disk was driven by a speed controllable motor to rotate against the stationary cylinder. The cylinder was held by a jig which connected to the upper part through a shaft. This design allows the cylindrical surface aligning to the flat surface of the disk automatically. The load was applied by dead weight. Friction force was obtained by measuring the deformation of the arm. In order to minimize the influences from the complicated friction modifier additives in most current commercial lubricants, light paraffin oil was used as the lubricant. Its viscosity is 0.0228 Pa s at 40 °C. One percent ZDDP was added to the oil as anti-wear agent to avoid severe wear during friction test.

The tests were conducted at the loads of 5–30 N, and rotational speeds of 10, 40, 70, and 100 rpm. The cylinder contacted the disk at the average radius of 20 mm, so the corresponding sliding speeds were 0.02, 0.08, 0.15, and 0.21 m/s, respectively. In order to minimize the effect of wear on friction, the tests were conducted by the sequence from high speed to low speed, and from low load to high load at each speed. At each test condition, the friction test was conducted for 30 s; the data after 10 s were calculated to obtain average friction coefficient.

## 2.3. Experimental results

Fig. 4 shows the friction coefficients of untextured specimen at different loads and sliding speeds. Fig. 5 was the replot of the data

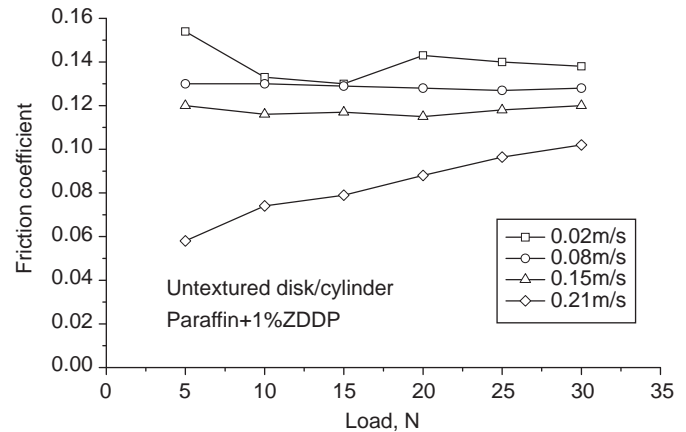


**Fig. 4.** Friction coefficients of untextured specimen.

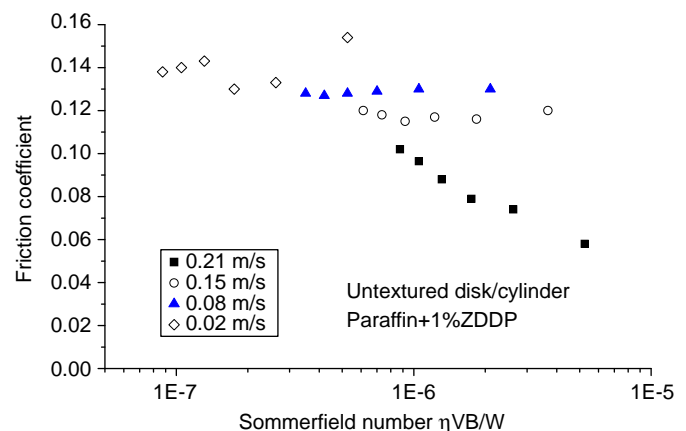


**Fig. 5.** Stribeck curve of the untextured specimen.

in Fig. 4 with X coordinate of Sommerfeld number  $\eta VB/W$ , where  $\eta$  is the viscosity of the lubricant,  $V$  is the sliding speed,  $B$  is the contact length between the cylindrical and plane surfaces, and  $W$  is the normal load. The data obtained from different sliding speeds could not present a typical Stribeck curve. That was because the wear occurred during the tests. Test at low sliding speed was conducted later, so that the effect of wear raised the friction coefficients of low sliding speed to a higher position in this figure. The friction coefficients at the sliding speed of 0.21 m/s were in the range from 0.06 to 0.10, indicating that it was in mixed lubrication regime. And at the other speeds, the friction coefficients increased to above 0.11, showing that boundary lubrication played a dominant role after wear occurred. This phenomenon also happened for textured specimen as shown in Fig. 6. Therefore, we would mainly discuss the experimental data at the sliding speeds of 0.15 and 0.21 m/s. The worn surface of the textured specimen after the tests is shown in Fig. 7.

Figs. 8 and 9 show the effect of dimple size on the friction coefficient between the cylinder and brass disk. The experimental data in Fig. 8 were obtained at 0.21 m/s, which was the first test speed, so that the wear effect is the minimum. It is shown that dimple diameter has an effect on friction coefficient. Compared with untextured specimen, the specimens with dimple diameter of 40 and 60  $\mu\text{m}$  have the friction coefficients higher than that of untextured specimen. They increased friction coefficient at an average rate of about 19.9% and 30.1%, respectively. Only the specimen with dimple diameter of 20  $\mu\text{m}$  had lower friction coefficient at load range from 10 to 30 N. It decreased the friction

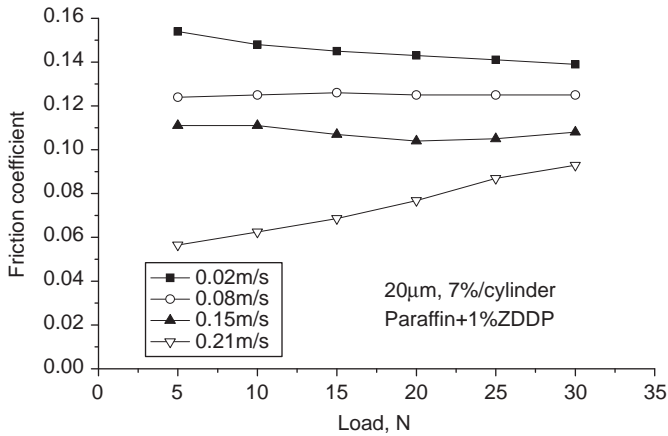


Fig. 6. Friction coefficients of the specimen with the dimples of 20 µm in diameter, 7% in area density, and 0.03 in depth over diameter ratio.

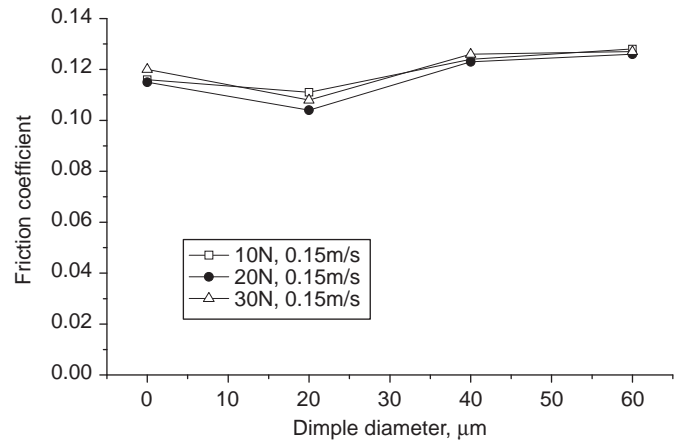


Fig. 9. Dimple diameter effect on friction coefficient at the sliding speed of 0.15 m/s.

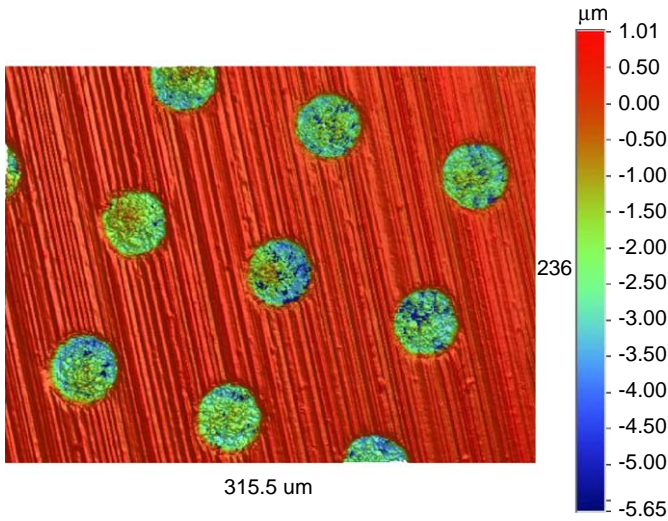


Fig. 7. Optical profiler measurement of the worn surface of brass disk after test.

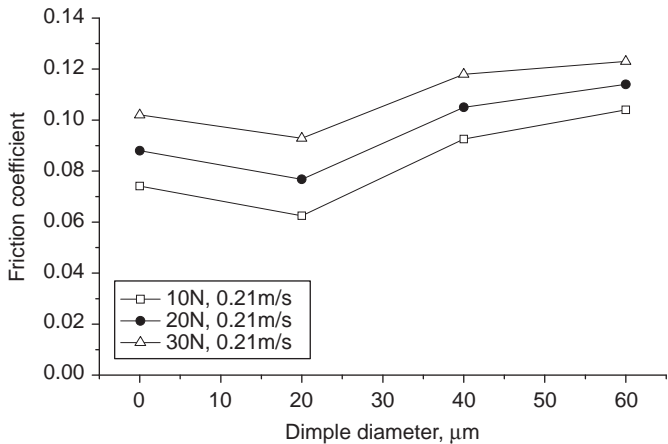


Fig. 8. Dimple diameter effect on friction coefficient at the sliding speed of 0.21 m/s.

15.6% at the load of 10 N, 12.7% at 20 N, and 8.9% at 30 N. These friction reduction rates are not as much as that of parallel surfaces in the previous research [7], indicating that it is difficult to decrease friction by the surface texture at line contact condition.



Fig. 10. The image of the cylinder after test.

Such effects of dimple size could also be found while sliding speed was decreased to 0.15 m/s as shown in Fig. 9. When the sliding speed was decreased to 0.08 m/s, all the friction coefficients were above 0.12, and there seems no obvious surface texture effect on friction. This is due to the wear on the contact surfaces.

Fig. 10 shows the image of the cylindrical surface after test. There was no obvious wear on the surface of cylinder. The black material deposited behind the contact line should be something like tribochemical product generated during the sliding test. From the image of the tribochemical product, we could find that the real contact length was not as long as the whole length of the cylinder. This may be due to the curvature of bearing roller used in this test. The real contact length could be measured as about 4 mm. Therefore, by the contact length, load, and radius of the cylinder, the half-width of contact  $b$  could be calculated by Hertz theory:

$$b = \sqrt{\frac{2PR}{\pi E^*}}$$

where  $R$  and  $E^*$  are the reduced radius of contact and the contact modulus,  $P$  is the force per unit length of magnitude.

The contact width  $2b$  is  $16.9\mu\text{m}$  by the load of  $10\text{N}$ , and  $29.3\mu\text{m}$  by the load of  $30\text{N}$ . Therefore, the experiment results show that the dimple diameter equivalent or smaller than contact width decreased friction coefficient, and dimple diameter much larger than the contact width would result in the increase of friction.

### 3. Numerical analysis

As shown in the experiment results, the effect of surface texture on friction is different for the patterns with different dimple sizes, although they have the same depth over diameter ratio  $h/d$ , which is the most important parameter for the additional hydrodynamic lubrication effect between parallel surfaces. This raises the questions how important the micro-hydrodynamic effect is under line contact condition, and how dimple size affects the micro-hydrodynamic pressure generated between the cylindrical and plane surfaces.

Therefore, in order to qualify the hydrodynamic effect with fast calculation and low-cost computer, a user-friendly commercial finite element software, ANSYS 10.0, is used for analysis.

#### 3.1. Methodology

The “contact” between the surfaces of the disk and the cylinder is simplified to that shown in Fig. 11. We assume only one dimensional flow through the bearing. Two surfaces are separated by a lubricant film with minimum thickness of  $h_{\text{min}}$ . The fluid is an incompressible Newtonian liquid with a constant viscosity  $\eta$ . Both the surfaces remain rigid. The lower surface is stationary, with or without dimple in the “contacting” area. The cylinder moves horizontally with a constant speed of  $V$ , so that micro-hydrodynamic effect would occur between the two surfaces. The hydrodynamic pressure increases on the right half side while pressure drops approximately to zero on the left half side with the assumption of cavitations. The average positive pressure on the cylindrical surface represents the load carrying capacity of these two surfaces.

The fluid flow and pressure variation along the bearing width were not taken into account. Of course it is not a real 3D simulation and will introduce a certain error, but it saves computing time without altering the general trend for textured and untextured surfaces.

Two kinds of dimples were used in the numerical simulation. One was a small dimple with diameter  $d_1 = 30\mu\text{m}$ , depth  $h_1 = 1\mu\text{m}$ , and length for calculation  $L_1 = 100\mu\text{m}$ . Another was a relative big dimple with dimple diameter  $d_2 = 90\mu\text{m}$ , depth  $h_2 = 3\mu\text{m}$ , and length for calculation  $L_2 = 300\mu\text{m}$ . Both small and

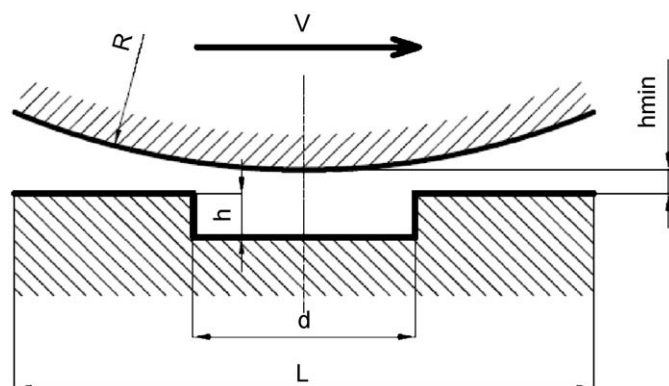


Fig. 11. Contact geometry.

big dimples have the same depth over diameter ratio  $h/d$  of  $0.03$ , the same area density (percentage of surface area occupied by dimples)  $r$  of  $7\%$ . These parameters of dimple pattern are effective for the generation of additional hydrodynamic pressure between the contact of parallel sliding surfaces [7].

The dimensions of the dimple used in numerical simulation are not the same as those for experiments. This is because we want to use integer to simplify the meshing process of finite element analysis.

The following input data were selected to investigate hydrodynamic effect:

viscosity of lubricant:  $\eta = 0.0228\text{Pa}\cdot\text{s}$   
 density of lubricant:  $804\text{kg}/\text{m}^3$   
 sliding speed:  $V = 0.1\text{m}/\text{s}, 0.5\text{m}/\text{s}$   
 minimum film thickness:  $h_{\text{min}} = 1\mu\text{m}$   
 radius of cylinder:  $R = 0.2\text{--}56\text{mm}$

Since cavitation is assumed to occur in the diverging region of each dimple, there should be zero pressure position between two dimples. Therefore, the pressure at the entrance and exit of the “contact” shown in Fig. 11 was assumed to be zero. The numerical simulation was carried out in this way to obtain the positive pressure distribution over the calculation length  $L$ . The average pressure generated by a dimple was then calculated and used as an index to evaluate the load carrying capacity of these two surfaces in this research.

#### 3.2. Results and discussion

Figs. 12 and 13 present the average hydrodynamic pressure generated between the cylinder and the disk surfaces. Fig. 12 is the comparison of a flat surface and a surface textured with the small dimple at sliding speeds of  $0.1$  and  $0.5\text{m}/\text{s}$ . It is shown that the textured surface is better on hydrodynamic pressure than that of flat surface. Radius of the cylinder has obvious influence on the hydrodynamic pressure between the surfaces. There is an optimal value of cylinder radius around  $1.0\text{mm}$  for hydrodynamic effect in this case. In the radius range up to this optimal value, the hydrodynamic pressure increases while radius increases for both the surfaces with and without dimple. When the radius is larger than the optimal value, both the surfaces with and without dimple have the hydrodynamic pressure decrease along the increase of cylinder radius. The average hydrodynamic pressure of untextured surface decreases faster than that of textured

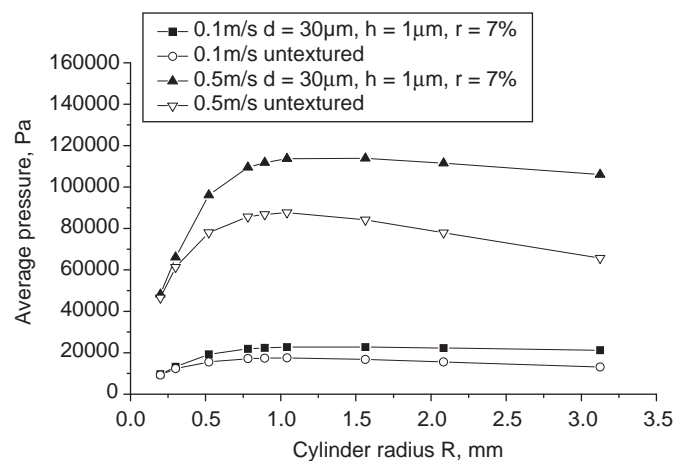


Fig. 12. Comparison of hydrodynamic pressure by untextured surface and textured surface with dimple diameter of  $30\mu\text{m}$ .

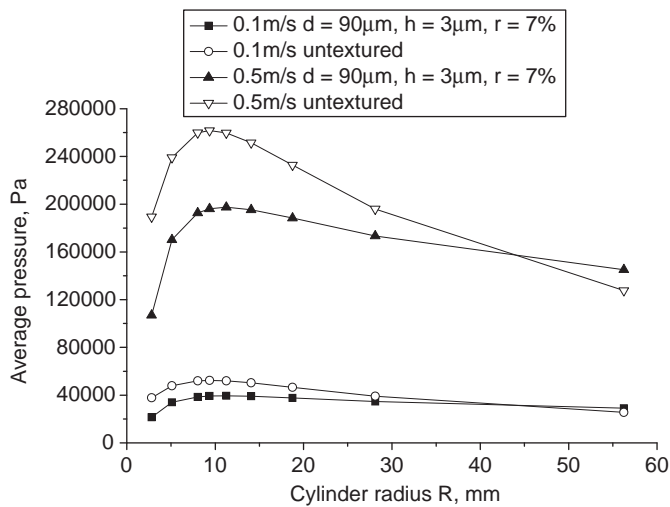


Fig. 13. Comparison of hydrodynamic pressure by untextured surface and textured surface with dimple diameter of 90  $\mu\text{m}$ .

surface, so that the curves of textured and untextured would not intersect while the cylinder radius increases further. It means the textured surface would be always better than untextured surface in this figure. High sliding speed would generate high hydrodynamic pressure, but there is not obvious change for the optimal value of cylinder radius.

Fig. 13 is the comparison of hydrodynamic pressure by a flat surface and by the textured surface with the dimple of 90  $\mu\text{m}$  in diameter at sliding speeds of 0.1 and 0.5 m/s. As mentioned above, the area density  $r$  and depth over diameter ratio  $h/d$  of this dimple is the same as that of the small dimple. There are several differences compared to Fig. 12. Because of the increase of dimple diameter, the optimal value of the cylinder radius also increased to the value around 9 mm. The curves of the flat and textured surfaces intersect around the cylinder radius of 45 mm. In range of the cylinder radius up to 45 mm, the hydrodynamic pressure generated by the dimpled surface is lower than that of the flat surface, while the cylinder radius is larger than 45 mm; the average hydrodynamic pressure of textured surface would be higher than that of the flat surface.

Therefore, the pattern with small dimples is easy to obtain hydrodynamic pressure higher than untextured surface. For the pattern with big dimple, it needs a much larger cylinder radius to obtain hydrodynamic pressure higher than untextured surface.

#### 4. Conclusions

Experiments and numerical simulations were carried out to investigate the dimple size effect on friction coefficient and load carrying capacity of the oil lubricated line contact.

(1) The frictional tests of the brass disk sliding against a stationary cylindrical surface of bearing steel were conducted. The brass disks were textured by the patterns of dimples with the same area density, the same depth over diameter ratio, and diameter of 20, 40, and 60  $\mu\text{m}$ . The results show that only

the pattern with dimple diameter of 20  $\mu\text{m}$  presented the effect of friction reduction.

(2) The numerical simulation results suggest that the radius of cylinder and the dimple size are the critical issues for the hydrodynamic effect in the case of line contact. The pattern with small dimples is easy to obtain hydrodynamic pressure higher than untextured surface. For the pattern with big dimples, it needs a much larger cylinder radius to obtain hydrodynamic pressure higher than that of untextured surface.

#### Acknowledgements

We would like to acknowledge the National Nature Science Foundation of China (NSFC) (no. 50675101), National High-tech R&D Program (no. 2006AA04Z321), and Science Foundation of Jiangsu province (no. BK2007529) for their financial supports.

#### References

- Bechert DW, et al. Fluid mechanics of biological surfaces and their technological application. *Naturwissenschaften* 2000;87:157–71.
- Barthlott W, Neinhuis C. Purity of the sacred lotus, or escape from contamination in biological surfaces. *Planta* 1997;202:1–8.
- Willis E. Surface finish in relation to cylinder liners. *Wear* 1986;109(1–4):351–66.
- Hamilton DB, Walowit JA, Allen CM. A theory of lubrication by micro-irregularities. *Journal of Basic Engineering* 1966;88(1):177–85.
- Etsion I, Kligerman Y, Halperin G. Analytical and experimental investigation of laser-textured mechanical seal faces. *Tribology Transactions* 1999;42(3):511–6.
- Wang X, et al. The effect of laser texturing of SiC surface on the critical load for the transition of water lubrication mode from hydrodynamic to mixed. *Tribology International* 2001;34(10):703–11.
- Wang X, et al. Loads carrying capacity map for the surface texture design of SiC thrust bearing sliding in water. *Tribology International* 2003;36(3):189–97.
- Brajdic-Mitidieri P, et al. CFD analysis of a low friction pocketed pad bearing. *Journal of Tribology—Transactions of the ASME* 2005;127(4):803–12.
- Etsion I, et al. Experimental investigation of laser surface textured parallel thrust bearings. *Tribology Letters* 2004;17(2):295–300.
- Etsion I. State of the art in laser surface texturing. *Journal of Tribology—Transactions of the ASME* 2005;127:248–53.
- Suh NP, Moseleh M, Howard PS. Control of friction. *Wear* 1994;175(1–2):151–8.
- Ranjan R, et al. Laser texturing for low-flying-height media. *Journal of Applied Physics* 1991;69(8):5745–7.
- Wang X, et al. Optimization of the surface texture for silicon carbide sliding in water. *Applied Surface Science* 2006;253(3):1282–6.
- Blatter A, et al. Lubricated sliding performance of laser-patterned sapphire. *Wear* 1999;232:226–30.
- Wang X, Hsu S. Surface texturing: a new design principle for friction reduction under boundary lubrication condition. In: *International tribology conference*. Kobe: The Japanese Society of Tribologists; 2005.
- Mourier L, et al. Transient increase of film thickness in micro-textured EHL contacts. *Tribology International* 2006;39(12):1745–56.
- Krupka I, Hartl M. The effect of surface texturing on thin EHD lubrication films. *Tribology International* 2007;40(7):1100–10.
- Krupka I, Hartl M. Experimental study of microtextured surfaces operating under thin-film EHD lubrication conditions. *Journal of Tribology—Transactions of the ASME* 2007;129(3):502–8.
- Wakuda M, et al. Effect of surface texturing on friction reduction between ceramic and steel materials under lubricated sliding contact. *Wear* 2003;254:356–63.
- Wang QJ, Zhu D. Virtual texturing: modeling the performance of lubricated contacts of engineered surfaces. *Journal of Tribology—Transactions of the ASME* 2005;127(4):722–8.
- Pettersson U, Jacobson S. Friction and wear properties of micro textured DLC coated surfaces in boundary lubricated sliding. *Tribology Letters* 2004;17(3):553–9.
- Costa HL, Hutchings IM. Hydrodynamic lubrication of textured steel surfaces under reciprocating sliding conditions. *Tribology International* 2007;40(8):1227–38.